


## Research Article

# Bifurcation Analysis and Exact Wave Solutions for the Double-Chain Model of DNA

Taher S. Hassan <sup>1,2</sup>, A.A. Elmandouh <sup>2</sup>, Adel A. Attiya <sup>1,2</sup> and Ahmed Y. Khedr<sup>3,4</sup>

<sup>1</sup>Department of Mathematics, College of Science, University of Ha'il, Ha'il 2440, Saudi Arabia

<sup>2</sup>Department of Mathematics, Faculty of Science, Mansoura University, Mansoura 35516, Egypt

<sup>3</sup>Department of Computer Science, University of Ha'il, Ha'il, Saudi Arabia

<sup>4</sup>Systems and Computer Engineering Department, Al-Azhar University, Cairo, Egypt

Correspondence should be addressed to A.A. Elmandouh; aelmandouh@kfu.edu.sa

Received 20 December 2021; Revised 26 January 2022; Accepted 1 April 2022; Published 11 May 2022

Academic Editor: Fairouz Tchier

Copyright © 2022 Taher S. Hassan et al. This is an open access article distributed under the Creative Commons Attribution License, which permits unrestricted use, distribution, and reproduction in any medium, provided the original work is properly cited.

This work aims to study analytically the nonlinear model for deoxyribonucleic acid (DNA). Based on the complete discrimination and direct method, some new wave solutions are introduced. These solutions are sorted into solitary, periodic, kink (antikink), and singular solutions. Moreover, a part of them is illustrated graphically. Based on Hamilton concepts, we study the bifurcation and phase portrait for the Hamilton system corresponding to the model under consideration.

## 1. Introduction

Deoxyribonucleic acid (DNA) molecule carries the information for living beings that is required to live and propagate themselves. The nonlinear model for deoxyribonucleic acid (DNA) is attractive for the study because its properties can be investigated precisely by experiments gathering both the physical methods and biological tools [1]. In 1953, Watson and Crick [2] initially discovered the double helix construction of DNA; in spite of that, it is not easy until now to find a specific mathematical model that involved all its characteristics. The reason is its complicated structure and the existence of several motions such as the torsional, transverse, and longitudinal motions [3]. However, the existence of several motions of the DNA on thoroughly distinct time scales becomes aidable to model a few of these that predominate in the given time scale range. The idea that was introduced by Davydov [4] in his pioneer works related to the theoretical studies of the nonlinear characteristics of DNA has been firstly utilized by Englander and coauthors in 1980 to investigate dynamics of DNA regarding the nitrogen rotational motion [5]. This idea has been further developed in several subsequent works. For instance, Yomosa proposed a

model of the dynamics plane of the base rotator [6], and this study was followed by Takeno and Homma who got better this model by considering the degree of freedom describing base rotations in the plane perpendicular to the helical axis around the structure of the backbone [7]. The denaturation process in which the base transverse motion along the hydrogen bond is regarded was investigated by Peyrard and Bishop [8]. Two kinds of internal motions, which have been proposed by Muto et al., contribute mainly to the denaturation process of DNA. These motions are longitudinal motions over the backbone and transverse motions over the hydrogen bond [9]. This model has been developed and improved in several works in order to study distinct motions and construct solitary wave-type solutions [10–14]. These waves acquire their significance from their ability to transmit energy without losing, i.e., the energy is conserved [8, 15], and moreover, they explicate the long-range interaction of kink solitons in the double chain [16, 17] and transcription regulation [18].

Taking into account some acceptable approximations from the point of biological science, the two equations describe a DNA model with double chains consisting of elastic two long homogeneous strands. These strands

characterize two polynucleotide chains of DNA molecules attached by an elastic membrane which represents the hydrogen bonds between the base pair of two chains. The dynamical nonlinear system characterizing the double-chain model of DNA takes the form [19, 20]

$$\begin{aligned} I_{tt} - e_1^2 I_{xx} &= a_1 I + b_1 IJ + c_1 I^3 + d_1 IJ^2, \\ J_{tt} - e_2^2 I_{xx} &= a_2 J + b_2 I^2 + c_2 I^2 J + d_2 J^3 + m_0, \end{aligned} \quad (1)$$

where  $I$  refers to the longitudinal displacement difference between the top and bottom wires, while  $J$  indicates the transverse displacements between the upper and lower strands, and  $e_i, a_i, b_i, c_i, d_i$ , and  $m_0$ ,  $i = 1, 2$ , are constants given by

$$\begin{aligned} e_1 &= \pm \frac{R_1}{\rho}, \\ e_2 &= \pm \frac{R_2}{\rho}, \\ a_1 &= \pm \frac{2\mu}{\rho\sigma h} (h - l_0), \\ a_2 &= \pm \frac{2\mu}{\rho\sigma}, \\ b_1 &= 2b_2 = \frac{2\sqrt{2}\mu l_0}{\rho\sigma h^2}, \\ c_1 &= c_2 = \frac{-2\mu l_0}{h^3 \rho\sigma}, \\ d_1 &= d_2 = \frac{4\mu l_0}{h^3 \rho\sigma}, \\ m_0 &= \frac{\mu\sqrt{2}}{\rho\sigma} (h - l_0), \end{aligned} \quad (2)$$

where  $\rho, \sigma, R_1$ , and  $R_2$  refer to density of mass, area of cross section, Young's modulus, and density of the tension of each strand,  $\mu$  indicates the stiffness of the elastic membrane,  $h$  is the distance between the two strands, and  $l_0$  is the height of membrane in the equilibrium.

To transform the nonlinear system (1) into a single partial differential equation, we present

$$J = \alpha I + \beta, \quad (3)$$

where  $\alpha$  and  $\beta$  are two arbitrary constants, and furthermore, we assume  $\beta = h/\sqrt{2}$  and  $R_1 = R_2$ . Thus, the linear system (1) is reduced to

$$I_{tt} - e_1^2 I_{xx} = f_3 I^3 + f_2 I^2 + f_1 I, \quad (4)$$

where  $f_i$  are arbitrary constants introduced for suitability, and they are given by

$$\begin{aligned} f_3 &= \frac{\omega_0}{h^3} (4\alpha^2 - 2), \\ f_2 &= \frac{6\sqrt{2}\alpha\omega_0}{h^2}, \\ f_1 &= \frac{6\omega_0}{h} - \frac{2\omega_0}{l_0}, \\ \omega_0 &= \frac{l_0\mu}{\sigma\rho}. \end{aligned} \quad (5)$$

The nonlinear model (1) has been investigated in several works. Riccati parameterized factorization method has been applied in [20] to construct some solitary wave solutions for the DNA model (1). The  $\Phi^6$ -model expansion method has been utilized in [21] to construct some solutions which are assorted into solitary, kink, and singular waves. Some solitary wave solutions for the double-chain model of DNA have been introduced and discussed [19]. Some exact wave solutions of this model have been constructed by using Conte's Painlevé truncation expansion and Pickering's truncation expansion [22]. Some bounded wave solutions for this model such as bell-shaped solitary waves and periodic waves have been formulated based on the method of the dynamical systems [23]. The generalized exponential rational function method has been applied to introduce exact form solutions and solitonic structures for this model [24].

Despite the wide variety of methods used to find wave solutions to nonlinear PDEs, the problem under study has a simple history, for instance, the bifurcation analysis [25–34], sine-Gordon expansion method [35, 36], Hirota bilinear technique [37],  $G'/G$  method [38–40], differential transform method (DTM), homotopy perturbation method (HPM) [41], Lie symmetry method [42], homotopic analysis method [43], trigonometric function series method [44], modified mapping method and extended mapping method [45], modified trigonometric function series method [46], tanh-coth expansion method and Jacobi function expansion method [47], and Jacobi elliptic function expansion method [48], and for more different techniques, see [49–53].

In this work, we are interested in constructing some traveling wave solutions for the nonlinear model (1) which is equivalent to building a wave solution for the reduced equation (1). We apply the complete discriminant system in addition to determining the intervals of permitted real propagations. The significance of finding these intervals enables us to construct only real wave solutions, and furthermore, for the same constraints on the system's parameters, there are several intervals of possible real wave propagations. Hence, the missing of such study in previous works leads to missing some wave solutions and the appearance of complex solutions. The bifurcation analysis is introduced which plays an important role in determining the types of the solutions before constructing them. We are also interested in studying the influence of the system's parameters on the solutions.

This work is organized as follows: Section 2 involves the reduction of the DNA model to ordinary differential equations and using the complete discrimination method to construct some traveling wave solutions for equation (1). Section 3 contains the study of some dynamical properties of equation (1) by employing the complete discrimination and Hamiltonian concepts. Section 4 is a graphic representation of some of the obtained solutions. Furthermore, it examines the influence of the one-parameter changing on the solutions keeping the other parameters fixed. Section 4 is a collection and the summary of the obtained results.

### 2. Exact Wave Solutions

Applying the wave transformation  $I(x, t) = u(\zeta)$ ,  $\zeta = kx - \omega t$ , to equation (4), we obtain

$$u'' = \frac{f_3}{\omega^2 - k^2 e_1^2} u^3 + \frac{f_2}{\omega^2 - k^2 e_1^2} u^2 + \frac{f_1}{\omega^2 - k a^2 e_1^2} u, \tag{6}$$

where  $k$  is a constant that specifies the cosine of angle of propagation with  $\zeta$ -axis and  $\omega$  is an arbitrary constant that characterizes the speed of the wave and  $\omega^2 - k^2 e_1^2 \neq 0$ . For simplicity, we insert

$$u(\zeta) = p(\zeta) - \frac{f_2}{3f_3}, \tag{7}$$

into equation (6), and we get

$$p''(\zeta) = 2n_4 p^3(\zeta) + n_2 p(\zeta) + \frac{n_1}{2}, \tag{8}$$

where ' indicates derivatives with respect to  $\zeta$  and  $n_i$ ,  $i = 2, 3, 4$ , are constants introduced for suitability and they are given by

$$\begin{aligned} n_4 &= \frac{f_3}{2(\omega^2 - k^2 e_1^2)}, \\ n_2 &= \frac{f_2^2 - 3f_3 f_1}{3f_3(k^2 e_1^2 - \omega^2)}, \\ n_1 &= \frac{2f_3(9f_1 f_2 - 2f_2^2)}{27f_3^2(k^2 e_1^2 - \omega^2)}. \end{aligned} \tag{9}$$

Integrating both sides of equation (8) with respect to  $p$ , we obtain

$$p'^2 = n_4(p^4 + \gamma_2 p^2 + \gamma_1 p + \gamma_0), \tag{10}$$

where  $\gamma_i$  are arbitrary parameters. Separating the variables, we obtain the differential form

$$d\zeta = \frac{dp}{\sqrt{n_4 F_4(p)}}, \tag{11}$$

where

$$F_4(p) = p^4 + \gamma_2 p^2 + \gamma_1 p + \gamma_0, \tag{12}$$

in which

$$\begin{aligned} \gamma_2 &= \frac{n_2}{n_4}, \\ \gamma_1 &= \frac{n_1}{n_4}. \end{aligned} \tag{13}$$

To integrate both sides of equation (11), the range of the parameters is required to be determined. The cause for this is that different values of the parameters imply different solutions to the integral. Hence, the key steps are to find the range of these parameters and consequently integrate both sides of equation (11). There are many tools utilized to find these ranges of parameters. In this work, we will apply a complete discrimination system for a polynomial. This method is a natural generalization of the discrimination  $\Delta = b^2 - 4ac$  for the quadratic polynomial  $ax^2 + bx + c$ , but it becomes difficult to calculate it for the higher degree polynomials. This problem had been solved with aid of computer algebra programs by Yang et al. by presenting an algorithm to compute the complete discrimination system for polynomial [54]. The complete discrimination system for the quartic polynomial  $F_4(p) = p^4 + \gamma_2 p^2 + \gamma_1 p + \gamma_0$  is given in [55], and it admits the form

$$\begin{aligned} D_1 &= 4, \\ D_2 &= -\gamma_2, \\ D_3 &= -2\gamma_2^3 + 8\gamma_2\gamma_0 - 9\gamma_1^2, \\ E_2 &= 9\gamma_2^2 - 32\gamma_2\gamma_0, \\ D_4 &= -\gamma_2^3\gamma_1^2 + 4\gamma_0\gamma_2^4 + 36\gamma_2\gamma_1^2 - 32\gamma_2^2\gamma_0^2 - \frac{27}{4}\gamma_1^4 + 64\gamma_0^4. \end{aligned} \tag{14}$$

We study eight cases that describe different types of the roots for polynomial (12). To avoid confounding, we collect the classification of all the different types of the roots of the polynomial  $F_4(p)$  by utilizing the discriminant system in Table 1. Furthermore, we integrate only on certain intervals for  $p$  in which  $n_4 F_4(p)$  is positive in order to get real solutions.

**2.1. Case 1.** Polynomial (12) has four real roots which are equal to zero if  $D_2 = D_3 = D_4 = 0$ . Hence, it is written as  $F_4(p) = p^4$ . Assuming  $-\infty < p < 0$  and  $p(\zeta_0) = -\infty$  and integrating (11), we obtain

$$I(x, t) = -\frac{1}{\sqrt{n_4}(kx + \omega t - \zeta_0)} - \frac{\sqrt{2}ah}{2a^2 - 1}, \tag{15}$$

and consequently, we have

$$J(x, t) = \alpha \left[ -\frac{1}{\sqrt{n_4}(kx + \omega t - \zeta_0)} - \frac{\sqrt{2}ah}{2a^2 - 1} \right] + \beta. \tag{16}$$

Solutions (15) and (16) are singular solutions, and their singularity points lie on the plane  $kx + ct - \zeta_0 = 0$ .

TABLE 1: Types of the roots of the polynomial  $F_4(p)$ .

No.	Conditions on the discriminant system	Types of the roots for $F_4(p)$
1	$D_2 = D_3 = D_4 = 0$	All roots are equal to zero
2	$D_3 = D_4 = E_2 = 0$	Two real roots: one is triple and the other is simple
3	$D_3 = D_4 = 0, E_2 > 0$	Two double roots
4	$D_2 > 0, D_3 > 0, D_4 > 0$	Four real roots
5	$D_4 = 0, D_2 D_3 < 0$	One double root and two complex conjugate roots
6	$D_4 < 0, D_2 D_3 > 0$	Two real roots and two complex conjugate roots
7	$D_2 D_3 \leq 0, D_4 > 0$	Two conjugate complex roots
8	$D_2 > 0, D_3 > 0, D_4 = 0$	Four real roots: one double and others simple

2.2. *Case 2.* If  $D_3 = D_4 = E_2 = 0$ , then the quartic polynomial (12) has two real roots: one is simple and the other is triple. Hence, it can be expressed as  $F_4(p) = (p - p_1)^3(p + 3p_1)$ , where  $p_1$  is assumed to be positive, i.e.,  $p_1 > 0$ . We consider two subcases according to  $n_4$  is positive or negative:

- (i) For  $n_4 > 0$ , the possible interval for real propagation is  $p \in ] - \infty, -3p_1[ \cup ]p_1, \infty[$ . Thus, if we choose  $p < -3p_1$ , assume  $p(\zeta_0) = -\infty$ , and integrate both sides of equation (11), we obtain

$$\sqrt{n_4} \int_{\zeta_0}^{\zeta} d\zeta = \int_{-\infty}^p \frac{dp}{(p - p_1)\sqrt{(p - p_1)(p + 3p_1)}} \quad (17)$$

It follows

$$p(\zeta) = p_1 - \frac{p_1}{p_1 \sqrt{n_4}(\zeta - \zeta_0) + 1} + \frac{1}{\sqrt{n_4}(\zeta - \zeta_0)}. \quad (18)$$

Thus, the solution of equation (1) becomes

$$\begin{aligned} I(x, t) &= p_1 - \frac{p_1}{p_1 \sqrt{n_4}(\zeta - \zeta_0) + 1} + \frac{1}{\sqrt{n_4}(\zeta - \zeta_0)} - \frac{f_2}{3f_3}, \\ J(x, t) &= \alpha \left[ p_1 - \frac{p_1}{p_1 \sqrt{n_4}(\zeta - \zeta_0) + 1} + \frac{1}{\sqrt{n_4}(\zeta - \zeta_0)} - \frac{f_2}{3f_3} \right] + \beta. \end{aligned} \quad (19)$$

Similarly, we can calculate the solution if  $p \in ]p_1, \infty[$ .

- (ii) If  $n_4 < 0$ , the possible interval for  $p$  to obtain real propagation is  $p \in ] - 3p_1, p_1[$ . Thus, we assume  $p(\zeta_0) = -3p_1$  and integrate both sides of equation (11), and we get

$$I(x, t) = p_1 - \frac{4p_1}{1 + 4n_4 p_1^2 (\zeta - \zeta_0)^2} - \frac{f_2}{3f_3}, \quad (20)$$

$$J(x, t) = \alpha \left[ p_1 - \frac{4p_1}{1 + 4n_4 p_1^2 (\zeta - \zeta_0)^2} - \frac{f_2}{3f_3} \right] + \beta.$$

Both solutions (19) and (20) are singular solutions for equation (1).

2.3. *Case 3.* The polynomial  $F_4(p)$  has two double real zeros, namely,  $\pm p_1$ , where  $p_1 > 0$ , if  $D_3 = D_4 = 0, E_2 > 0, D_2 > 0$ . Hence, it can be introduced as  $F_4(p) = (p^2 - p_1^2)^2$ . We consider the following two cases in which  $n_4$  is either positive or negative.

- (i) If  $n_4 > 0$ , the intervals for real propagation are  $p < -p_1, -p_1 < p < p_1$ , and  $p > p_1$ . If we consider the case in which  $p < -p_1$  and assume  $p(\zeta_0) = -\infty$ , equation (11) gives

$$\sqrt{n_4} \int_{\zeta_0}^{\zeta} d\zeta = \int_{-\infty}^p \frac{dp}{p^2 - p_1^2}. \quad (21)$$

It follows

$$p = -p_1 \coth(p_1 \sqrt{n_4} (\zeta - \zeta_0)). \quad (22)$$

Using equations (7) and (3), we obtain a wave solution for equation (1) in the form

$$I(x, t) = -p_1 \coth(p_1 \sqrt{n_4} (\zeta - \zeta_0)) - \frac{f_2}{3f_3}, \quad (23)$$

$$J(x, t) = \alpha \left[ -p_1 \coth(p_1 \sqrt{n_4} (\zeta - \zeta_0)) - \frac{f_2}{3f_3} \right] + \beta.$$

When  $p > p_1$ , equation (1) has the same solution shown in equation (23) if  $p_1 \rightarrow -p_1$ . Similarly, if we choose  $p \in ] - p_1, p_1[$  and assume  $p(\zeta_0) = 0$ , equation (1) has a solution in the form

$$I(x, t) = -p_1 \tanh(p_1 \sqrt{n_4} (\zeta - \zeta_0)) - \frac{f_2}{3f_3}, \quad (24)$$

$$J(x, t) = \alpha \left[ -p_1 \tanh(p_1 \sqrt{n_4} (\zeta - \zeta_0)) - \frac{f_2}{3f_3} \right] + \beta.$$

- (ii) The case in which  $n_4 < 0$  is excluded since  $n_4 F_4(p) < 0$  for all  $p \in \mathbb{R}$ .

2.4. *Case 4.* The polynomial  $F_4(p)$  has four real zeros, namely,  $p_1, p_2, p_3, -(p_1 + p_2 + p_3)$ , where we assumed  $0 < p_1 < p_2 < p_3$  if  $D_2 > 0, D_3 > 0, D_4 > 0$ . Therefore, it takes the form  $F_4(p) = (p - p_1)(p - p_2)(p - p_3)(p +$

$p_1 + p_2 + p_3$ ). Now, we consider the two cases  $n_4 > 0$  and  $n_4 < 0$ , individually:

- (i) When  $n_4 > 0$ , the possible intervals of  $p$  for real propagation are  $p < -(p_1 + p_2 + p_3)$ ,  $p_1 < p <$

$p_2$ , and  $p > p_3$ . If we choose  $p < -(p_1 + p_2 + p_3)$  and assume  $p(\zeta_0) = -(p_1 + p_2 + p_3)$ , equation (11) becomes

$$\sqrt{n_4} \int_{\zeta_0}^{\zeta} d\zeta = \int_{-(p_1+p_2+p_3)}^p \frac{dp}{\sqrt{(p-p_1)(p-p_2)(p-p_3)(p+p_1+p_2+p_3)}} \tag{25}$$

It implies to

$$p = p_1 - \frac{(p_1 - p_3)(2p_1 + p_2 + p_3)}{p_1 - p_3 + (p_1 + p_2 + 2p_3)\text{sn}^2(\Omega_1(\zeta - \zeta_0), k_1)}, \quad \zeta_0 < \zeta < \zeta_1, \tag{26}$$

where  $\Omega_1 = 1/2\sqrt{n_4(p_3 - p_1)(p_1 + 2p_2 + p_3)}$ ,  $k_1 = \sqrt{((p_2 - p_1)(p_1 + p_2 + 2p_3))/((p_3 - p_1)(p_1 + 2p_2 + p_3))}$ , and  $\zeta_1 = (1/\Omega_1)K(k_1)$ .  $K(k_1)$  is a

complete elliptic integral of the first type [56]. Using equations (7) and (3), we obtain a new traveling wave solution for equation (1) in the form

$$\Omega_1(x, t) = p_1 - \frac{(p_1 - p_3)(2p_1 + p_2 + p_3)}{p_1 - p_3 + (p_1 + p_2 + 2p_3)\text{sn}^2(\Omega_1(\zeta - \zeta_0), k_1)} - \frac{f_2}{3f_3}, \tag{27}$$

$$J(x, t) = \alpha \left[ p_1 - \frac{(p_1 - p_3)(2p_1 + p_2 + p_3)}{p_1 - p_3 + (p_1 + p_2 + 2p_3)\text{sn}^2(\Omega_1(\zeta - \zeta_0), k_1)} - \frac{f_2}{3f_3} \right] + \beta.$$

If we select  $p_1 < p < p_2$ , postulate  $p(\zeta_0) = p_1$ , and follow the same procedures, we will obtain a new traveling wave solution for equation (1) in the form

$$I(x, t) = -p_1 - p_2 - 2p_3 + \frac{(p_1 + 2p_2 + p_3)(2p_1 + p_2 + 2p_3)}{p_1 + 2p_2 + p_3 + (p_1 - p_2)\text{sn}^2(\Omega_1(\zeta - \zeta_0), k_1)} - \frac{f_2}{3f_3}, \tag{28}$$

$$J(x, t) \alpha \left[ -p_1 - p_2 - 2p_3 + \frac{(p_1 + 2p_2 + p_3)(2p_1 + p_2 + 2p_3)}{p_1 + 2p_2 + p_3 + (p_1 - p_2)\text{sn}^2(\Omega_1(\zeta - \zeta_0), k_1)} - \frac{f_2}{3f_3} \right] + \beta,$$

where  $\zeta_0 < \zeta < \zeta_1$ . Also, if we elect  $p > p_3$  and suppose  $p(\zeta_0) = p_3$ , we will get a new wave solution for equation (1) in the form

$$I(x, t) = p_2 + \frac{(p_2 - p_3)(p_1 + 2p_2 + p_3)}{(p_1 + p_2 + 2p_3)\text{sn}^2(\Omega_1(\zeta - \zeta_0), k_1)} - \frac{f_2}{3f_3}, \tag{29}$$

$$J(x, t) = \alpha \left[ p_2 + \frac{(p_2 - p_3)(p_1 + 2p_2 + p_3)}{(p_1 + p_2 + 2p_3)\text{sn}^2(\Omega_1(\zeta - \zeta_0), k_1)} - \frac{f_2}{3f_3} \right] + \beta,$$

where  $\zeta_0 < \zeta < \zeta_1$ .

- (ii) If  $n_4 < 0$ , the allowed intervals of  $p$  for real propagation are  $-p_1 - p_2 - p_3 < p < p_1$  or  $p_2 < p < p_3$ .

Thus, if we chose  $p_1 < p < p_3$  and assume  $p(\zeta_0) = -p_1 - p_2 - p_3$ , equation (11) takes the form

$$\sqrt{-n_4} \int_{\zeta_0}^{\zeta} d\zeta = \int_{-p_1-p_2-p_3}^p \frac{dp}{\sqrt{\sqrt{-(p-p_1)(p_2-p)(p_3-p)(p+p_1+p_2+p_3)}}} \quad (30)$$

It gives

$$p = p_3 + \frac{(p_1 - p_3)(p_1 + p_2 + 2p_3)}{p_3 - p_1 + (2p_1 + p_2 + p_3)\text{sn}^2(\Omega_2(\zeta - \zeta_0), k_2)}, \quad \zeta_0 < \zeta < \zeta_2, \quad (31)$$

where  $\Omega_2 = 1/2\sqrt{-n_4(p_3 - p_1)(2p_2 + p_1 + p_3)}$ ,  $k_2 = \sqrt{((p_3 - p_2)(2p_1 + p_2 + p_3)) / ((p_3 - p_1)(2p_2 + p_1$

$+ p_3))$ , and  $\zeta_2 = (1/\Omega_2)K(k_2)$ . Utilizing equations (7) and (3), we obtain a new solution for equation (1):

$$I(x, t) = p_3 + \frac{(p_1 - p_3)(p_1 + p_2 + 2p_3)}{p_3 - p_1 + (2p_1 + p_2 + p_3)\text{sn}^2(\Omega_2(\zeta - \zeta_0), k_2)} - \frac{f_2}{3f_3}, \quad (32)$$

$$J(x, t) = \alpha \left[ p_3 + \frac{(p_1 - p_3)(p_1 + p_2 + 2p_3)}{p_3 - p_1 + (2p_1 + p_2 + p_3)\text{sn}^2(\Omega_2(\zeta - \zeta_0), k_2)} \right] + \beta.$$

Similarly, if we select  $p_2 < p < p_3$  and assume  $p(\zeta_0) = p_2$ , we present a new wave solution for equation (1) in the form

$$I(x, t) = p_1 - \frac{(p_1 - p_2)(p_1 - p_3)}{p_1 - p_3 + (p_3 - p_2)\text{sn}^2(\Omega_2(\zeta - \zeta_0), k_2)} - \frac{f_2}{3f_3}, \quad (33)$$

$$J(x, t) = \alpha \left[ p_1 - \frac{(p_1 - p_2)(p_1 - p_3)}{p_1 - p_3 + (p_3 - p_2)\text{sn}^2(\Omega_2(\zeta - \zeta_0), k_2)} - \frac{f_2}{3f_3} \right] + \beta.$$

**2.5. Case 5.** The polynomial  $F_4(p)$  has one double real root and two conjugate complex roots if  $D_4 = 0$  and  $D_2D_3 < 0$ . Therefore, it takes the form  $F_4(p) = (p - p_1)^2(p - p_2)(p - p_2^*)$ , where \* refers to the complex conjugate and  $p_1 = -\text{Re}p_2$ . We consider the case in which  $n_4 > 0$ , and sequentially, the allowed intervals for real propagation are  $p < p_1$  or  $p > p_1$ . Choosing  $p > p_1$ , assuming  $p(\zeta_0) = \infty$ , and integrating both sides of equation (11), we obtain

$$p = p_1 + \frac{4p_1^2 + \rho^2}{-2p_1 + \rho \sinh\left(\sqrt{n_4(4p_1^2 + \rho^2)}(\zeta - \epsilon)\right)}, \quad (34)$$

where  $\epsilon = \zeta_0 - s(\text{inh}^{-1}(2p_1/\rho))/\sqrt{n_4(4p_1^2 + \rho^2)}$  is a new constant which is introduced for suitability and  $\rho = \text{Im}p_2$ . Employing equations (7) and (3), we obtain a solution for equation (1) in the form

$$I(x, t) = p_1 + \frac{4p_1^2 + \rho^2}{-2p_1 + \rho \sinh\left(\sqrt{n_4(4p_1^2 + \rho^2)} (\zeta - \epsilon)\right)} - \frac{f_2}{3f_3},$$

$$J(x, t) = \alpha \left[ p_1 + \frac{4p_1^2 + \rho^2}{-2p_1 + \rho \sinh\left(\sqrt{n_4(4p_1^2 + \rho^2)} (\zeta - \epsilon)\right)} - \frac{f_2}{3f_3} \right] + \beta. \tag{35}$$

It can be noted that the case in which  $n_4$  is negative does not work because  $F_4(p) \geq 0$  for all  $p \in \mathbb{R}$ .

2.6. Case 6. The polynomial  $F_4(p)$  has two real roots and two complex conjugate roots if  $D_4 < 0$  and  $D_2D_3 > 0$ . Hence, it can be written in the form  $F_4(p) = (p - p_1)(p - p_2)(p - p_3)(p - p_3^*)$ , where  $p_1 < p_2$  and  $\text{Re}p_3 = (1/2)(p_1 + p_2)$ . We consider the following:

(i) If  $n_4 > 0$ , then the permitted intervals for real propagation are  $p > p_2$  and  $p < p_1$ . Selecting  $p < p_2$

and  $p(\zeta_0) = p_2$  and integrating both sides of equation (11), we obtain

$$p = \frac{p_2B_1 - p_1A_1 + (p_2B_1 + p_1A_1)\text{cn}\left(\sqrt{n_4A_1B_1} (\zeta - \zeta_0), k_2\right)}{(A_1 + B_1)\text{cn}\left(\sqrt{n_4A_1B_1} (\zeta - \zeta_0), k_2\right) - (A_1 - B_1)}, \tag{36}$$

where  $k_2 = \sqrt{((A_1 + B_1)^2 - (p_2 - p_1)^2)/4A_1B_1}$  and  $A_1^2 = B_1^2 = (1/4)(p_1 - p_2)^2 + \text{Im}^2(p_3)$ . Taking into account equations (7) and (3), we obtain a novel wave solution for equation (1) in the form

$$I(x, t) = \frac{p_2B_1 - p_1A_1 + (p_2B_1 + p_1A_1)\text{cn}\left(\sqrt{n_4A_1B_1} (kx + \omega t - \zeta_0), k_2\right)}{(A_1 + B_1)\text{cn}\left(\sqrt{n_4A_1B_1} (\zeta - \zeta_0), k_2\right) - (A_1 - B_1)} - \frac{f_2}{3f_3},$$

$$J(x, t) = \alpha \left[ \frac{p_2B_1 - p_1A_1 + (p_2B_1 + p_1A_1)\text{cn}\left(\sqrt{n_4A_1B_1} (kx + \omega t), k_2\right)}{(A_1 + B_1)\text{cn}\left(\sqrt{n_4A_1B_1} (\zeta - \zeta_0), k_2\right) - (A_1 - B_1)} - \frac{f_2}{3f_3} \right] + \beta. \tag{37}$$

(ii) If  $n_4 < 0$ , then the allowed intervals of possible propagation are  $p_1 < p < p_2$ . Assuming  $p(\zeta_0) = p_1$

and integrating both sides of equation (11), we obtain

$$p = \frac{p_2B_2 + p_1A_2 + (p_1A_2 - p_2B_2)\text{cn}\left(\sqrt{-n_4A_2B_2} (\zeta - \zeta_0), k_3\right)}{B_2 + A_2 - (B_2 - A_2)\text{cn}\left(\sqrt{-n_4A_2B_2} (\zeta - \zeta_0), k_3\right)}, \tag{38}$$

where  $k_3 = \sqrt{((p_2 - p_1)^2 - (A_2 - B_2)^2)/4A_2B_2}$ ,  $A_2^2 = (1/4)(p_1 + 3p_2)^2 + \text{Im}^2p_3$ , and  $B_2^2 = (1/4)(3p_1 + p_2)^2 + \text{Im}^2p_3$ . Utilizing equations

(7) and (3), we construct a novel wave solution for equation (1) in the form

$$I(x, t) = \frac{p_2B_2 + p_1A_2 + (p_1A_2 - p_2B_2)\text{cn}\left(\sqrt{-n_4A_2B_2} (kx + \omega t - \zeta_0), k_3\right)}{B_2 + A_2 - (B_2 - A_2)\text{cn}\left(\sqrt{-n_4A_2B_2} (kx + \omega t - \zeta_0), k_3\right)} - \frac{f_2}{3f_3},$$

$$J(x, t) = \alpha \left[ \frac{p_2B_2 + p_1A_2 + (p_1A_2 - p_2B_2)\text{cn}\left(\sqrt{-n_4A_2B_2} (kx + \omega t - \zeta_0), k_3\right)}{B_2 + A_2 - (B_2 - A_2)\text{cn}\left(\sqrt{-n_4A_2B_2} (kx + \omega t - \zeta_0), k_3\right)} - \frac{f_2}{3f_3} \right] + \beta. \tag{39}$$

2.7. Case 7. The polynomial  $F_4(p)$  has two conjugate complex roots, namely,  $p_1, p_1^*, p_2, p_2^*$ , if  $D_2D_3 \leq 0$  and  $D_4 > 0$ . Therefore, it is expressed as  $F_4(p) = (p - p_1)(p - p_1^*)(p - p_2)(p - p_2^*)$ , where

$\text{Re}p_1 = -\text{Re}p_2$ . The permitted interval for real propagation for the case  $n_4 > 0$  is  $p \in \mathbb{R}$ . Thus, we follow similar steps as above and obtain a new traveling wave solution for equation (1) as

$$I(x, t) = \frac{\operatorname{Re} p_1 + \operatorname{Im} p_1 \delta + (\operatorname{Im} p_1 + \operatorname{Re} p_1 \delta) \operatorname{tn}((\sqrt{n_4}/2)(A_2 + B_2)(kx + \omega t - \zeta_0), k_4)}{\delta + \operatorname{tn}((\sqrt{n_4}/2)(A_2 + B_2)(kx + \omega t - \zeta_0), k_4)} - \frac{f_2}{3f_3},$$

$$J(x, t) = \alpha \left[ \frac{\operatorname{Re} p_1 + \operatorname{Im} p_1 \delta + (\operatorname{Im} p_1 + \operatorname{Re} p_1 \delta) \operatorname{tn}((\sqrt{n_4}/2)(A_2 + B_2)(kx + \omega t - \zeta_0), k_4)}{\delta + \operatorname{tn}((\sqrt{n_4}/2)(A_2 + B_2)(kx + \omega t - \zeta_0), k_4)} - \frac{f_2}{3f_3} \right] + \beta, \tag{40}$$

where  $A_2^2 = [\operatorname{Im} p_1 - \operatorname{Im} p_2]^2$ ,  $B_2^2 = [\operatorname{Im} p_1 - \operatorname{Im} p_2]^2 + 4\operatorname{Re}^2 p_1$ ,  $\delta^2 = (4\Re p_1^2 - (A_2 - B_2)^2) / ((A_2 + B_2)^2 - 4\Re p_1^2)$ , and  $k_4 = (2\sqrt{A_2 B_2}) / (A_2 + B_2)$ . It can be noted that the case in which  $n_4 < 0$  does not work because  $F_4(p) > 0$  for all  $p \in \mathbb{R}$ .

2.8. Case 8. The polynomial  $F_4(p)$  has four real roots in which one of them is double and the others are simple if  $D_2 > 0, D_3 > 0$ , and  $D_4 = 0$ . Hence, it takes the form  $F_4(p) = (p - p_1)^2(p - p_2)(p - p_3)$ , where  $p_1 < p_2 < p_3$  and

$p_3 = -(2p_1 + p_2)$ . We consider the two cases in which  $n_4$  is either positive or negative:

(i) If  $n_4 > 0$ , then the possible intervals for real propagation are  $p < p_1, p > p_3$ , and  $p_1 < p < p_2$ . With similar computations as in previous cases, we present the solution of equation (1) directly.

If we choose  $p > -(2p_1 + p_2)$  and assume  $p(\zeta_0) = -(2p_1 + p_2)$ , we have a new wave solution for equation (1) in the form

$$I(x, t) = -2p_1 - p_2 + 4(p_2 - p_1) \operatorname{sech} \left( \sqrt{n_4(-3p_1 - p_2)} (kx + \omega t - \zeta_0) - \frac{f_2}{3f_3} \right),$$

$$J(x, t) = \alpha \left[ -2p_1 - p_2 + 4(p_2 - p_1) \operatorname{sech} \left( \sqrt{n_4(-3p_1 - p_2)} (kx + \omega t - \zeta_0) - \frac{f_2}{3f_3} \right) \right] + \beta. \tag{41}$$

In similar calculations, we can calculate the wave solution for  $p < p_1$  and  $p_1 < p < p_2$ .

(ii) If  $n_4 < 0$ , the allowed interval for real propagation is  $p \in ]p_2, p_3[$ , and postulating  $p(\zeta_0) = p_2$ , we obtain a new wave solution for equation (1) in the form

$$I(x, t) = p_1 + \frac{(p_2 - p_1)(3p_1 + p_2)}{2p_1 + (p_1 + p_2) \cosh \sqrt{-n_4(3p_1 + p_2)}(p_1 - p_2)(kx - \omega t - \zeta_0)} - \frac{f_2}{3f_3},$$

$$J(x, t) = \alpha \left[ p_1 + \frac{(p_2 - p_1)(3p_1 + p_2)}{2p_1 + (p_1 + p_2) \cosh \sqrt{-n_4(3p_1 + p_2)}(p_1 - p_2)(kx - \omega t - \zeta_0)} - \frac{f_2}{3f_3} \right] + \beta. \tag{42}$$

### 3. Dynamic Properties

The aim of this section is to investigate some dynamic properties for equation (4) by investigating the bifurcation and phase portrait for the traveling wave system corresponding to equation (8) which takes the form

$$p' = z,$$

$$z' = 2n_4 \left( p^3 + \frac{\gamma_2}{2} p + \frac{\gamma_1}{4} \right). \tag{43}$$

System (43) is a Hamiltonian system with one degree of freedom related to Hamilton function:

$$\frac{1}{2} z^2 + V(p) = h, \tag{44}$$

where  $h$  is an arbitrary constant and

$$V(q) = -\frac{n_4}{2} (p^4 + \gamma_2 p^2 + \gamma_1 p), \tag{45}$$

is the potential function. It is well known that the equilibrium points for the Hamilton system (43) are also critical points for the potential function (45), i.e., they are the roots of

$$\frac{dV}{dp} = -2n_4 \left( p^3 + \frac{\gamma_2}{2} p + \frac{\gamma_1}{4} \right). \tag{46}$$

Thus, we use the discrimination of (46) to determine the number of equilibrium points. The discrimination of (46) is

$$\Delta = -\frac{1}{8} \left[ \frac{\gamma_1^2}{8} + \frac{\gamma_2^3}{27} \right]. \tag{47}$$

Now, let us determine the number of equilibrium points for the Hamilton system (43) and study the properties of its phase space. Thus, we need to define energy curve corresponding to



$$\mathcal{E}_h = \{(p, z) \in \mathbb{R}^2: z^2 = 2(h - V(p))\}. \quad (48)$$

It is well known that any orbit for the Hamilton system (43) is an energy curve on a certain level of the energy.

*Case 1.* The dynamical system (43) has a unique equilibrium point if  $dV/dp = 0$  has a unique real root. This happens in two cases which are studied individually:

- (i) If  $\Delta = 0$  and  $\gamma_2 = 0$ , then  $dV/dp = 0$  has one triple real root, i.e.,  $dV/dp = -2n_4 p^3$ . This shows  $(0, 0)$  is a unique equilibrium point for system (43) which is saddle if  $n_4 > 0$ , and it is center if  $n_4 < 0$ . The phase space for this case is outlined by Figures 1(a) and 1(b). The value of the energy at the equilibrium point  $(0, 0)$  is  $h_1 = V(0, 0) = 0$ . The following proposition describes Figure 1.
- (ii) If  $\Delta < 0$ , then  $dV/dp = 0$  has one real zero and two complex conjugate roots, i.e.,

$$\frac{dV}{dp} = -2n_4(p - a) \left[ \left( p + \frac{a}{2} \right)^2 + m^2 \right]. \quad (49)$$

It is clear that the point  $(a, 0)$  is a unique equilibrium point for the Hamilton system (43) and it is saddle if  $n_4 > 0$  and center if  $n_4 < 0$ . The phase space is clarified by Figures 2(a) and 2(b).

**Proposition 1.** The Hamiltonian system (43) has a unique equilibrium point  $(0, 0)$  if  $\gamma_1 = \gamma_2 = 0$ . If  $n_4 > 0$ , it is a saddle point and all the orbits are unbounded, see Figure 1(a). If  $n_4 < 0$ , system (43) has a family of bounded periodic orbits  $\{\mathcal{E}_h: h > h_1\}$  about the center point  $(0, 0)$  as outlined by Figure 1(b). A similar conclusion can be presented to describe Figure 2.

*Case 2.* If  $\Delta = 0$  and  $\gamma_2 < 0$ , then  $dV/dp = 0$  has two real roots: one is simple and the other is double. Thus, we write  $dV/dp = -2n_4(p - a)^2(p + 2a)$  and so  $(a, 0)$  and  $(-2a, 0)$  are two equilibrium points for system (43). It is clear that  $(a, 0)$  is a cusp while  $(-2a, 0)$  is a center if  $n_4 < 0$  and saddle if  $n_4 > 0$ . The phase portrait for this case is outlined in Figure 3. The following proposition gives a short description for the phase portrait for this case.

**Proposition 2.** The Hamiltonian system (43) has two equilibrium points  $E_1 = (a, 0)$  and  $E_2 = (-2a, 0)$ . If  $n_4 > 0$ , then  $E_1$  is cusp point while  $E_2$  is saddle, and furthermore, all the phase space orbits are unbounded as outlined in Figure 3(a). While if  $n_4 < 0$ ,  $E_1$  is a cusp and  $E_2$  is a center. The Hamilton system (43) has two bounded families of periodic orbits which are illustrated in green and blue and separated by the phase curve  $\{\mathcal{E}_h: h = V(a, 0)\}$  in red.

*Case 3.* If  $\Delta > 0$  and  $\gamma_2 < 0$ , then  $dV/dp$  has three real roots, i.e., it can be written as  $dV/dp = -2n_4(p - a)(p - b)(p + a + b)$ , where we assumed  $b > a > 0$ . Consequently, the dynamical system (43) has three equilibrium points  $(a, 0)$ ,  $(b, 0)$ , and  $(-a - b, 0)$ . If  $n_4 > 0$ , then  $(a, 0)$  is center and  $(b, 0)$  and  $(-a - b, 0)$  are saddle points. While if  $n_4 < 0$ ,

$(a, 0)$  is saddle point and the other two equilibrium points are center. The phase portrait for this case is described in Figures 4(a) and 4(b). We describe the phase portrait for the Hamiltonian system in the following proposition.

**Proposition 3.** If  $\Delta > 0$  and  $\gamma_2 < 0$ , then the Hamilton system (43) has three equilibrium points  $(a, 0)$ ,  $(b, 0)$ , and  $(-a - b, 0)$ . If  $n_4 > 0$ , there are two families of orbits  $\{\mathcal{E}_h: h \in ]V(a), V(b)[\}$  in green in which one of them is bounded and surrounded by the homoclinic orbit  $\{\mathcal{E}_h: h = V(2a)\}$  while the other family is unbounded. Moreover, all the other orbits are unbounded, see Figure 4(a) for more clarification. If  $n_4 < 0$ , system (43) has three equilibrium points in which one is a saddle and the others are centers. It has three bounded families of periodic orbits. Two of them in blue and green are periodic orbits around the two center points  $(2a, 0)$  and  $(-a - b, 0)$ , and they are separated by the homoclinic orbit in red  $\{\mathcal{E}_h: h = V(a)\}$ . The third one is a family of superperiodic orbits in brown  $\{\mathcal{E}_h: h > V(a)\}$  around the two centers points and lies outside the homoclinic orbit in red. For more details about superperiodic orbits, see, for example, [57].

The investigation of the type of the phase space orbits is helpful in determining the types of the solutions. For instance, the existence of periodic orbits, homoclinic orbits, and heteroclinic orbits for the traveling wave system (43) indicates the existence of periodic wave solutions, solitary, and kink solutions for equation (1). Furthermore, this analysis can be employed to construct the traveling wave solution by introducing the constraints on the coefficients of function (12). Consequently, we can prove the following theorem.

**Theorem 1.** Let  $I(x, t) = u(kx - \omega t)$  and  $J(x, t) = \alpha I(x, t) + \beta$  be a solution for the double-chain model of DNA (1), then

- (i) It is a periodic solution if
  - (a)  $n_4 < 0, h > 0, \Delta = 0 (\gamma_1 = \gamma_2 = 0)$ ,
  - (b)  $n_4 < 0, h > V(a, 0), \Delta < 0$ ,
  - (c)  $n_4 < 0,$   
 $\Delta = 0, \gamma_2 < 0, h \in ]V(-2a), V(a)[ \cup ]V(a), \infty[$ ,
  - (d)  $n_4 > 0, \Delta > 0, \gamma_2 > 0, h \in ]V(a), V(b)[$ ,
  - (e)  $n_4 < 0, \Delta > 0, \gamma_2 > 0, h \in ]V(a), \infty[$ ,
  - (f)  $n_4 < 0, \Delta > 0, \gamma_2 > 0, h \in$   
 $]V(a), \infty[ \cup ]V(b), V(a)[ \cup ]V(c), V(b)[$ .
- (ii) It is a solitary wave solution if  $n_4 < 0, \Delta > 0,$   
 $\gamma_2 < 0,$  and  $h = V(a)$ .
- (iii) It is a kink (antikink) solution if  $n_4 > 0, \Delta > 0,$   
 $\gamma_2 < 0,$  and  $h = V(b)$ .

#### 4. Graphic Interpretations

This section aims to illustrate some of the obtained solutions graphically. Moreover, we study the influence of the physical parameters on the obtained solutions by considering two

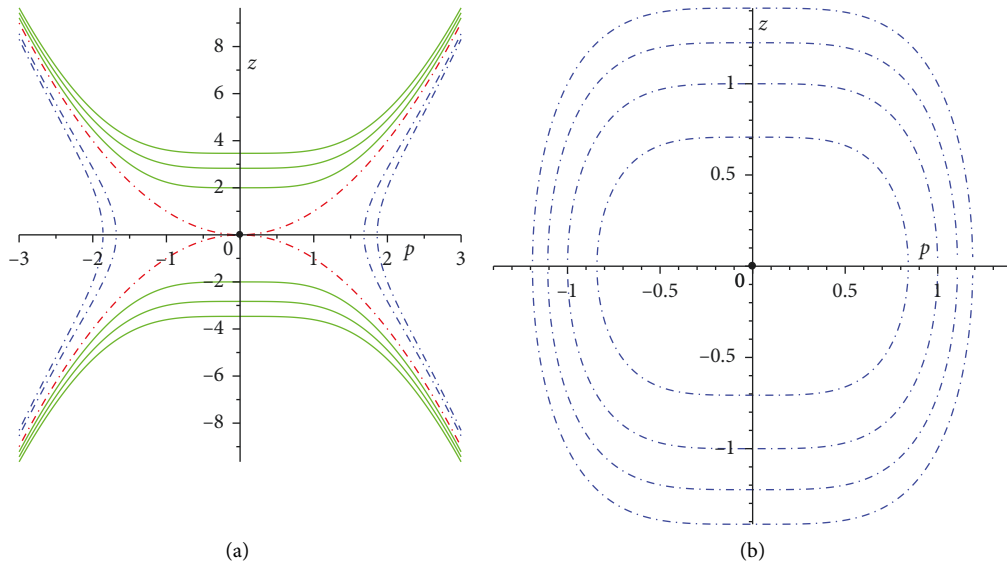


FIGURE 1: Phase portrait for the Hamilton system (43) for  $\gamma_1 = 0$  and  $\gamma_2 = 0$ . (a)  $n_4 = 1$  and (b)  $n_4 = -1$ .

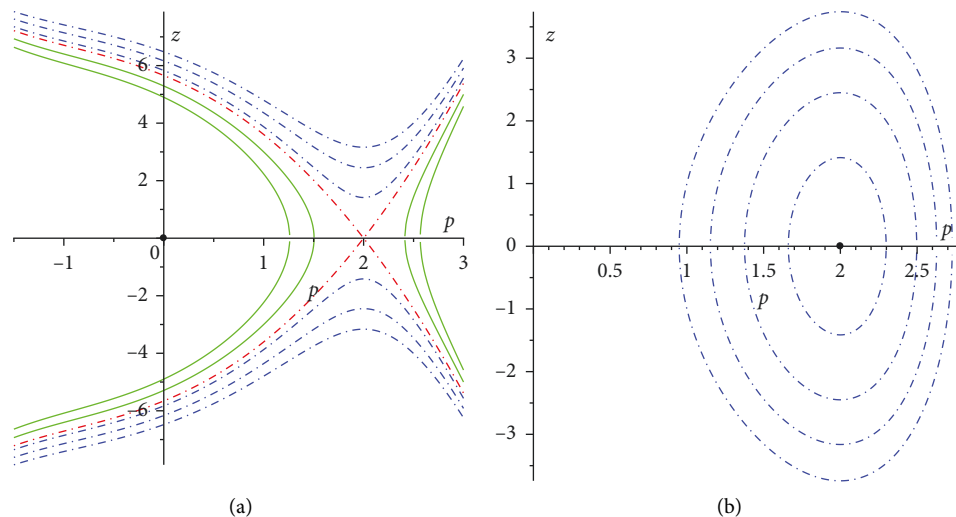


FIGURE 2: Phase portrait for the Hamilton system (43) for  $\Delta < 0$ . (a)  $n_4 = 1$ ,  $\gamma_1 = -16$ , and  $\gamma_2 = -4$ . (b)  $n_4 = -1$ ,  $\gamma_1 = -16$ , and  $\gamma_2 = -4$ .

types of solutions: one of them is kink solution and the other is periodic.

Figure 5 and 6 illustrates the kink solution (24) for different aspects. Figures 5(a) and 5(b) clarify the 3D and contour representation for the kink solution (24) when  $k = 1$ ,  $\omega = 2$ ,  $\sigma = 0.001$ ,  $\rho = 0.1$ ,  $\mu = 0.0001$ ,  $h = 0.002$ ,  $R_1 = 0.1$ , and  $l_0 = 0.002$ . Now, we illustrate graphically the influence of some parameters on the kink solution while the other parameters are fixed. Figure 6(a) illustrates the effect of the change of the distance between the two strands. It is remarkable the amplitude of solution (24) is decreased when the distance between the two strands is increased. Figure 6(b) clarifies the amplitude of the solution is increased when the stiffness of the elastic membrane is increased. Figure 6(c) clarifies the amplitude of the solution is decreased when the area of the

cross section of each strand is increased. Figure 6(d) outlines the amplitude of the kink solution (24) is increased when the height of the membrane in the equilibrium is increased (see Figure 7).

Now, we are going to clarify solution (28) graphically and study the influence of parameter changes on solution (28). Solution (28) is periodic as outlined in Figure 8(a), and its contour is illustrated in Figure 8(b). If the distance between the two strands is increased and the other parameters are fixed, the amplitude of the solution is unchanged but the width of the solution is increased as outlined in Figure 8(a). The amplitude of solution (28) is not affected by the changes in the stiffness of the elastic membrane, while the width of the solution is decreased when the stiffness of the elastic membrane is increased as clarified by Figure 8(d). If the area of the cross section of each strand is increased, then the

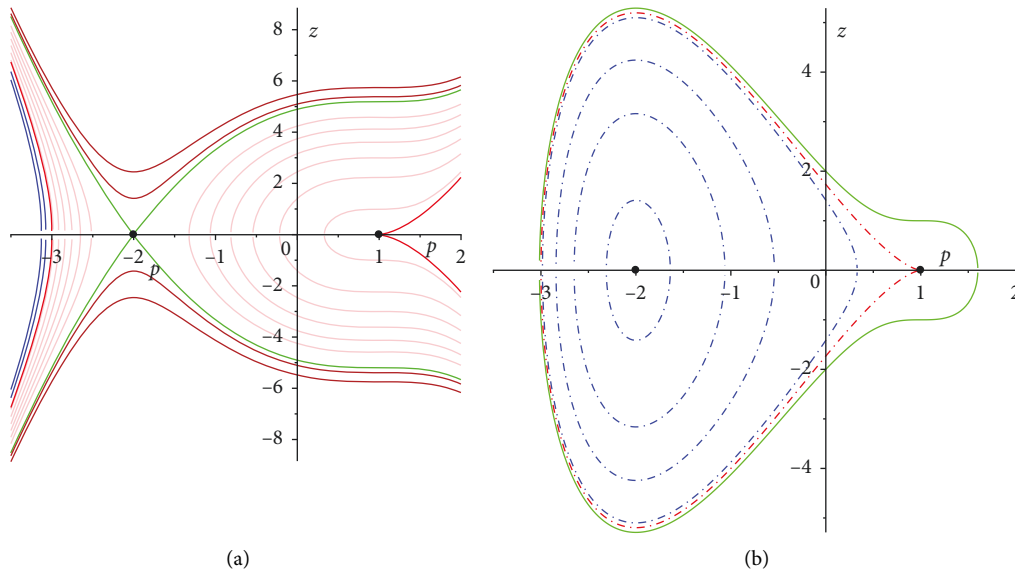


FIGURE 3: Phase portrait for the Hamilton system (43) for  $\Delta = 0$  and  $\gamma_2 < 0$ . (a)  $n_4 = 1$ ,  $\gamma_1 = 8$ , and  $\gamma_2 = -6$ . (b)  $n_4 = -1$ ,  $\gamma_1 = 8$ , and  $\gamma_2 = -6$ .

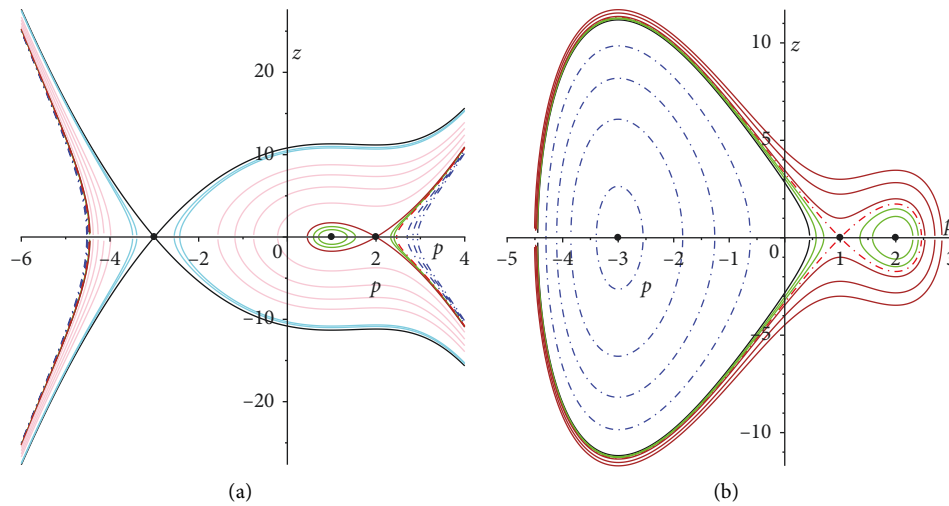


FIGURE 4: Phase portrait for the Hamilton system (43) for  $\Delta > 0$  and  $\gamma_2 < 0$ . (a)  $n_4 = 1$ ,  $\gamma_1 = 8$ , and  $\gamma_2 = -6$ . (b)  $n_4 = -1$ ,  $\gamma_1 = 8$ , and  $\gamma_2 = -6$ .

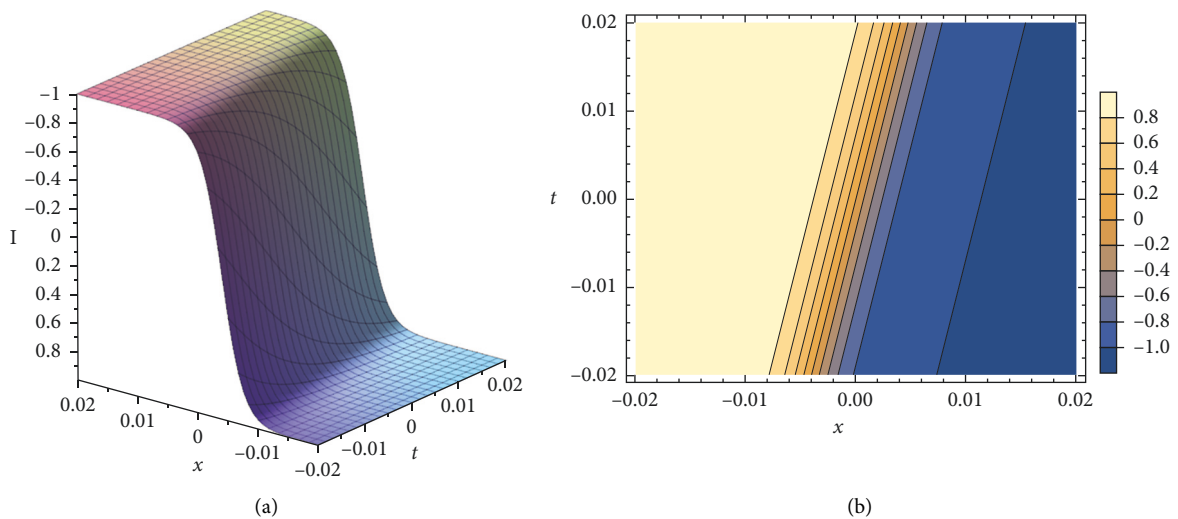


FIGURE 5: Graphic representation of solution (24) for  $R_1 = 0.1$ ,  $h = 0.002$ ,  $k = 1$ ,  $l_0 = 0.002$ ,  $\mu = 0.0001$ ,  $\omega = 2$ ,  $\rho = 0.1$ , and  $\sigma = 0.001$ . (a) 3D graphic and (b) 2D contour plot.

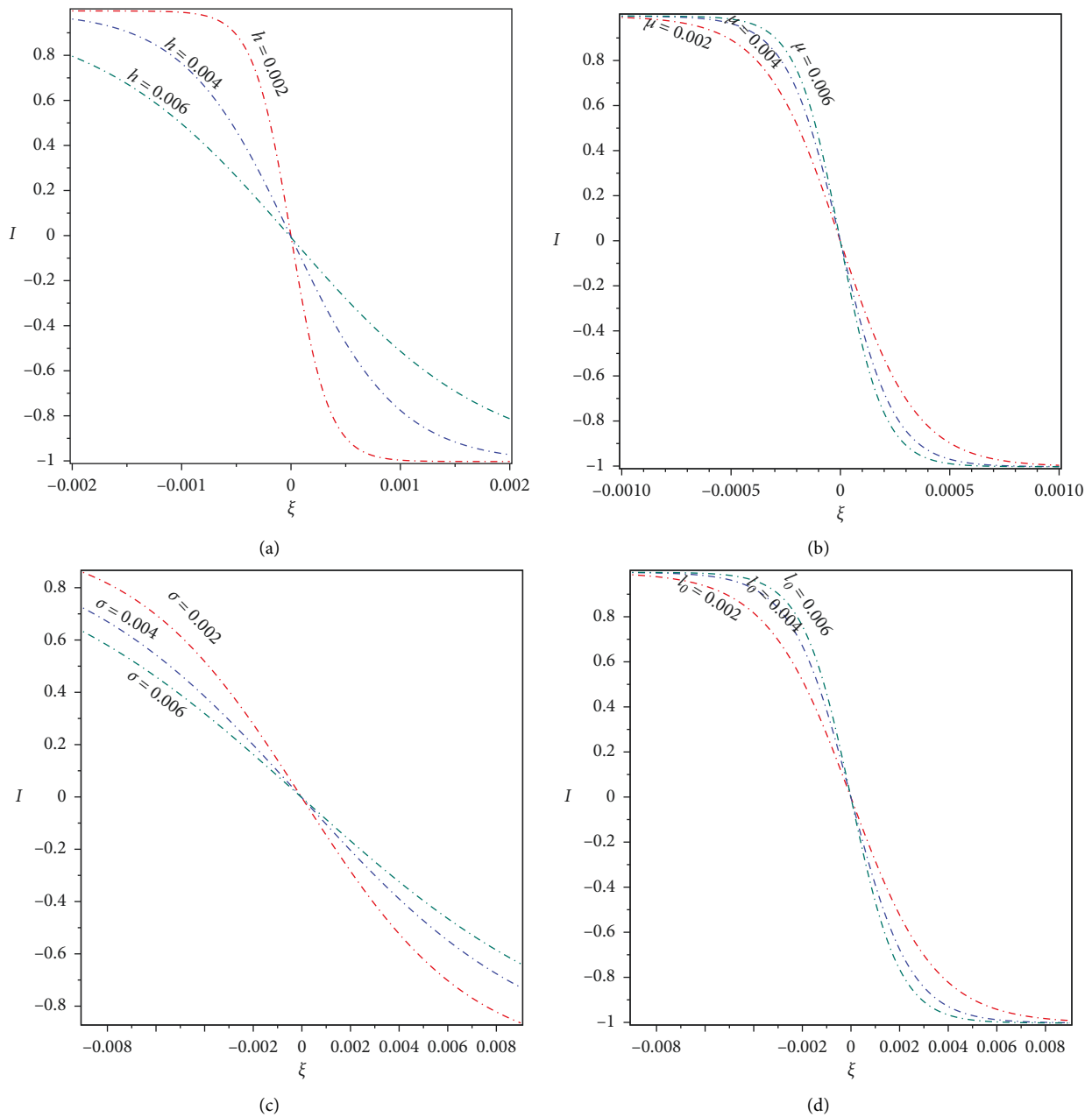


FIGURE 6: Parameters affecting solution (24): (a) changes in  $h$  for  $R_1 = 0.1, k = 1, l_0 = 0.001, \mu = 0.002, \rho = 0.1,$  and  $\sigma = 0.0001,$  (b) changes in  $\mu$  for  $R_1 = 0.1, h = 0.002, k = 1, l_0 = 0.001, \omega = 2, \rho = 0.1,$  and  $\sigma = 0.0001,$  (c) changes in  $\sigma$  for  $R_1 = 0.1, h = 0.002, k = 1, l_0 = 0.001, \mu = 0.0001, \omega = 0.1,$  and  $\rho = 0.1,$  and (d) changes in  $l_0$  for  $R_1 = 0.1, h = 0.002, k = 1, \sigma = 0.001, \rho = 0.1, \mu = 0.0001,$  and  $\omega = 2.$

amplitude keeps fixed while the width is increased, see Figure 8(d). Figure 9(b) outlines the amplitude of the periodic solution (28) is kept unchanged while its width is decreased when the height of the membrane in the equilibrium is increased. Figure 9(a) illustrates the influence of the superperiodic wave solution (39) due the changes in the stiffness of the elastic membrane. If the stiffness of the elastic membrane increases, the amplitude is kept unchanged while the width decreases. Figure 9(b) clarifies the influence of distance between the two strands on the superwave solution

(39). If distance between the two strands is increased, then the amplitude and the width of superwave solution (39) are increased.

It is worth mentioning that we can make the same study for the remaining obtained solutions. However, we only give the 3D graphic and the 2D counter for some solutions. The 3D graphic representation and the singularity plane are outlined in Figure 10(a), while Figure 10(b) illustrates the 2D contour of solution (15). Solution (37) is illustrated in Figure 11.

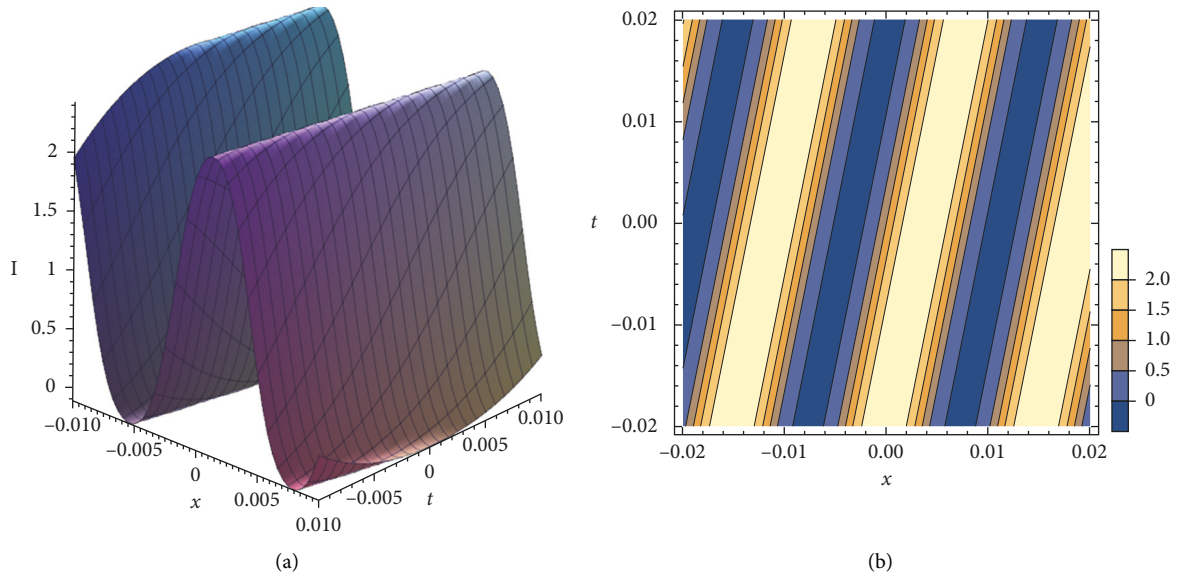


FIGURE 7: Graphic representation of solution (28) for  $R_1 = 0.1$ ,  $h = 0.002$ ,  $k = 1$ ,  $l_0 = 0.002$ ,  $\mu = 0.0001$ ,  $\omega = 0.2$ ,  $\rho = 0.1$ , and  $\sigma = 0.001$ . (a) 3D graphic and (b) 2D contour plot.

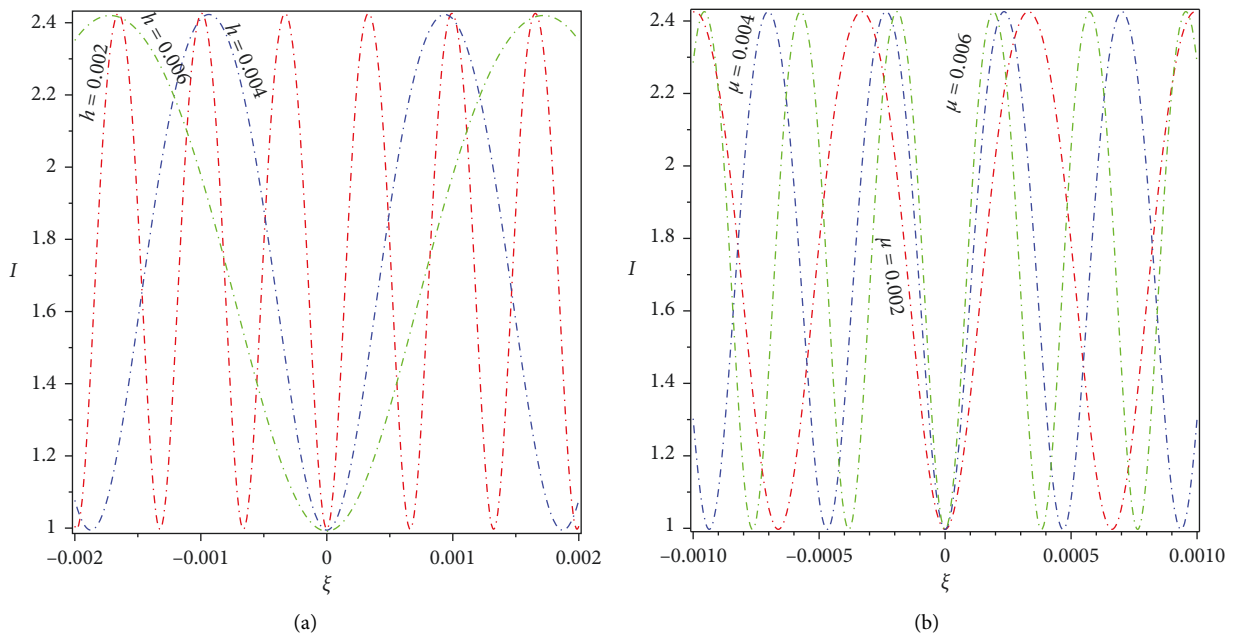


FIGURE 8: Continued.

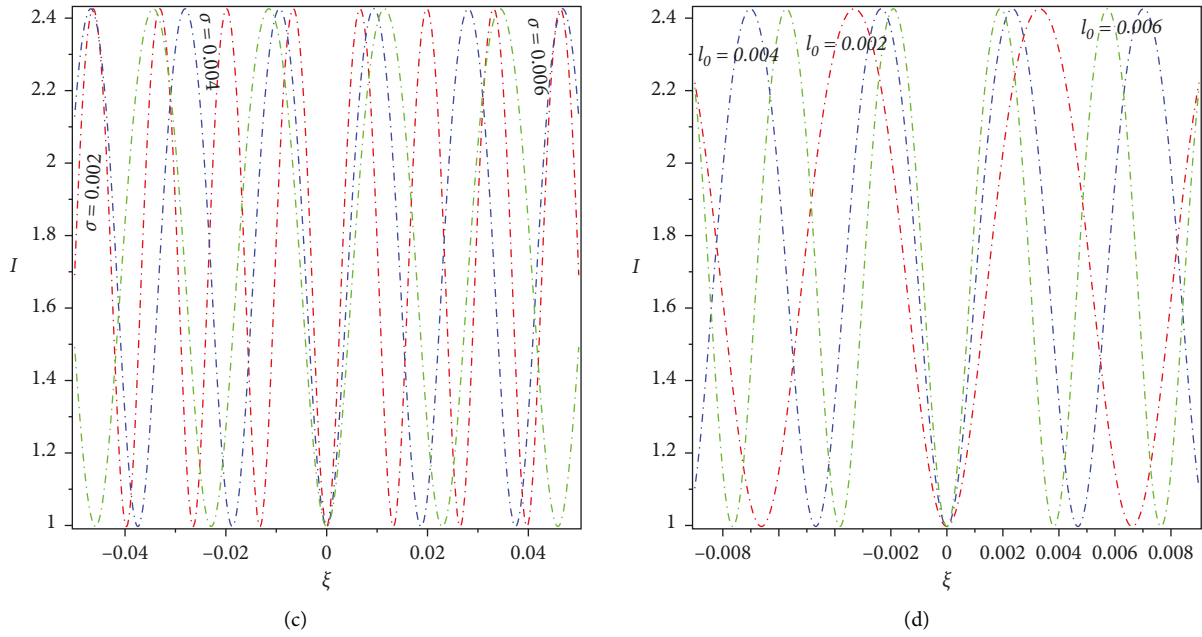


FIGURE 8: Parameters affecting solution (28): (a) changes in  $h$  for  $R_1 = 0.1$ ,  $k = 1$ ,  $l_0 = 0.001$ ,  $\mu = 0.002$ ,  $\omega = 2$ ,  $\rho = 0.1$ , and  $\sigma = 0.0001$ , (b) changes in  $\mu$  for  $R_1 = 0.1$ ,  $h = 0.002$ ,  $k = 1$ ,  $l_0 = 0.001$ ,  $\omega = 2$ ,  $\rho = 0.1$ , and  $\sigma = 0.0001$ , (c) changes in  $\sigma$  for  $R_1 = 0.1$ ,  $h = 0.002$ ,  $k = 1$ ,  $l_0 = 0.001$ ,  $\mu = 0.0001$ ,  $\omega = 2$ , and  $\rho = 0.1$ , and (d) changes in  $l_0$  for  $R_1 = 0.1$ ,  $h = 0.0002$ ,  $k = 1$ ,  $\mu = 0.0001$ ,  $\omega = 2$ ,  $\rho = 0.1$ , and  $\sigma = 0.001$ .

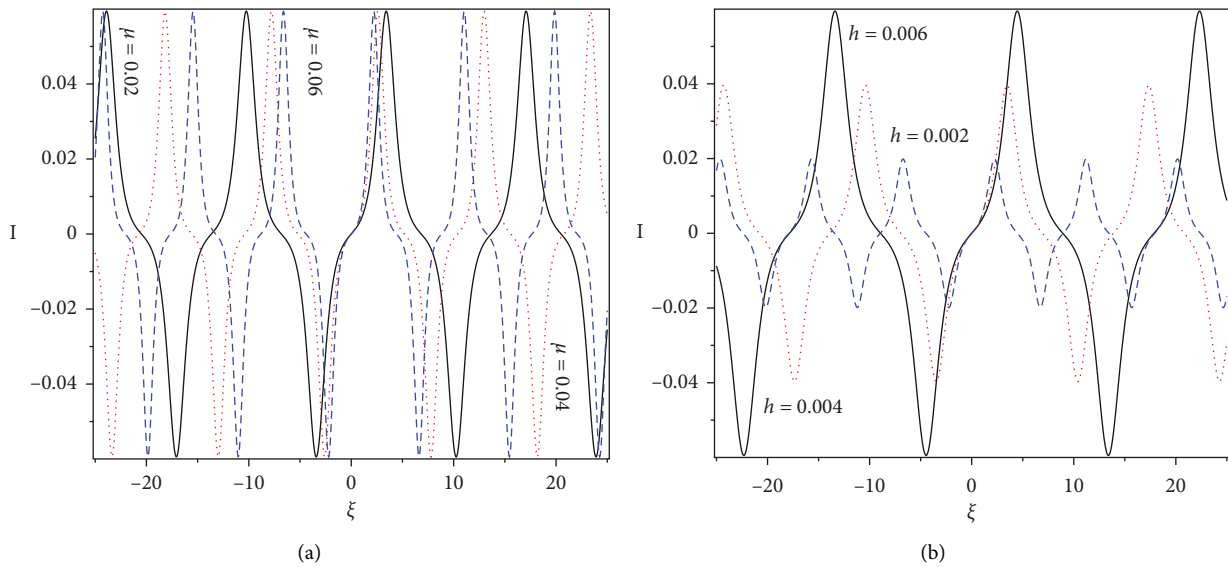


FIGURE 9: Parameters affecting the superwave solution (39): (a) changes in  $\mu$  for  $R_1 = 0.01$ ,  $\alpha = 0.8$ ,  $h = 0.006$ ,  $k = 1$ ,  $l_0 = 0.001$ ,  $\rho = 0.00002$ , and  $\sigma = 0.01$  and (b) changes in  $h$  for  $R_1 = 0.01$ ,  $\alpha = 0.8$ ,  $h = 0.006$ ,  $k = 1$ ,  $l_0 = 0.001$ ,  $\rho = 0.00002$ , and  $\sigma = 0.01$ .

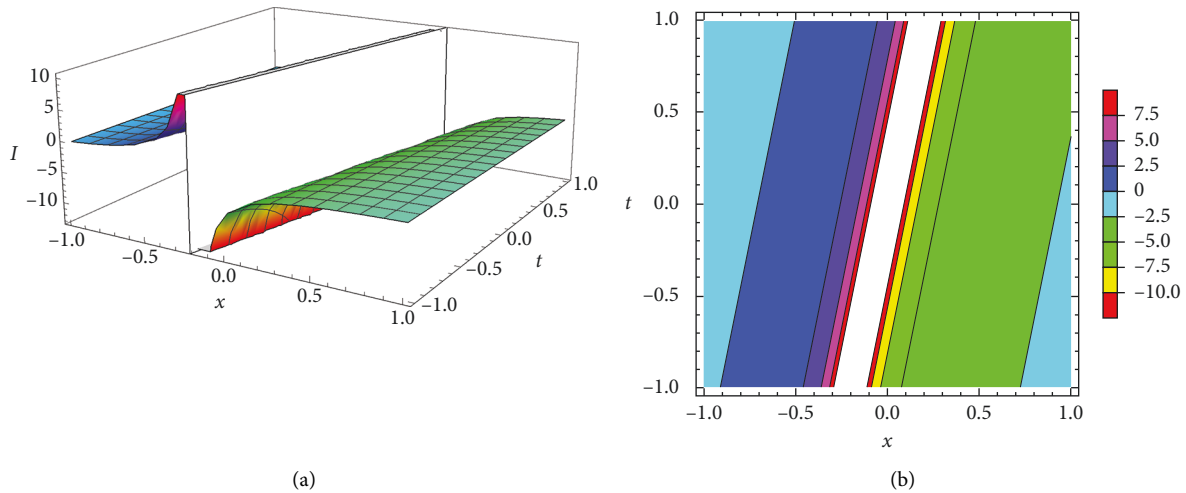


FIGURE 10: Graphic representation for the singular wave solution (15). (a) 3D graphic and (b) 2D contour.

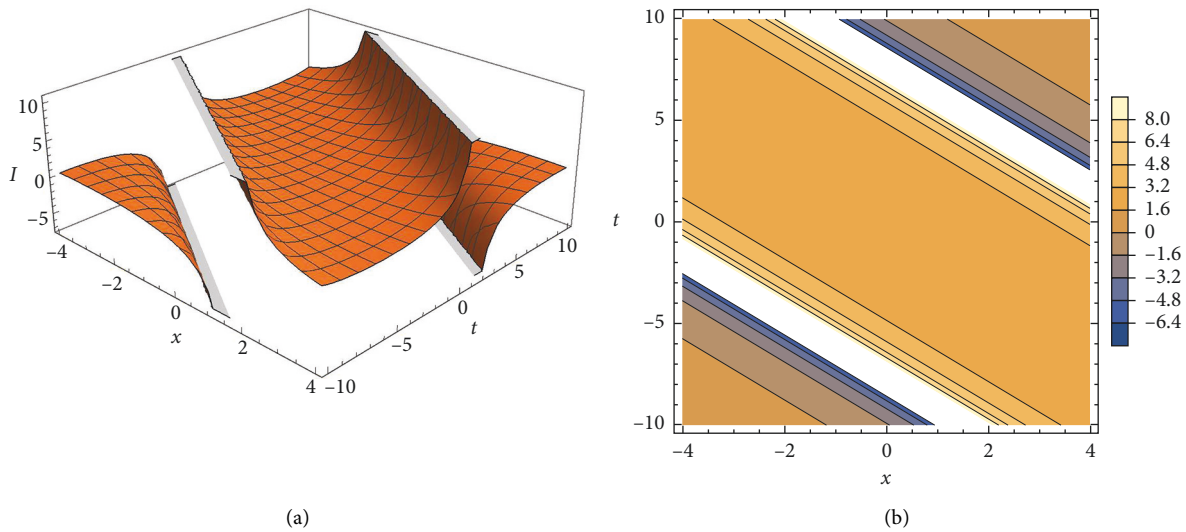


FIGURE 11: Graphic representation for the singular wave solution (37). (a) 3D graphic and (b) 2D contour.

### 5. Conclusion

This work is aimed to study analytically the double-chain model for deoxyribonucleic acid (DNA). A certain wave transformation has been applied to equation (1) to transform it into an ordinary differential equation. The integration of this equation reacquired some studies on the parameters. This study has been performed by applying the complete discrimination of the polynomial  $F_4(p)$ . Moreover, we have determined the possible interval of real propagations. Such study is more significant because the missing of such study implies to loss some solutions and also, give rise to complex solutions which are undesirable in real problems. For instance, there are several solutions corresponding to the same conditions on the discriminant system as outlined in Case 4. We have introduced new waves' solutions for equation (1). Let us compare the results obtained in the present article

with the well-known results obtained by other authors using different methods as follows: our results in a new double-chain model of DNA are new and different from those obtained in references [19–24]. We have studied the influence of some parameters such as the distance between the two strands, the stiffness of the elastic membrane, the area of the cross section of each strand, and the height of the membrane in the equilibrium. We have considered two types of solutions: one is kink (24) and the other is periodic (28). We have shown graphically the amplitude of the kink solution is decreased when the distance between the two strands or the area of the cross section of each strand is increased, while it is increased when the stiffness of the elastic membrane or the height of the membrane in the equilibrium is increased. For more clarification, see Figure 6. The amplitude of the periodic solution remains approximately unchanged when these physical parameters are



changed, but the width has been affected. The width is increased due to the increase of the distance between the two strands or the area of the cross section of each strand, while it is decreased as a result of increasing the stiffness of the elastic membrane or the height of the membrane in the equilibrium. For more illustrations, see Figure 10. From another point of view, this ODE has been expressed as a one-dimensional Hamiltonian system that describes the physical motion of a particle with one degree of freedom under the action of potential function  $V(p)$  given by (45). Based on the Hamiltonian concepts, we have studied some qualitative analyses such as phase portrait and bifurcation. The description of phase space has been presented through Propositions 1, 2, and 3. Moreover, these propositions contain the conditions for the existence of periodic and solitary wave solutions.

### Data Availability

No data were used to support the study.

### Conflicts of Interest

The authors declare that they have no conflicts of interest.

### Acknowledgments

This research has been funded by the Scientific Research Deanship at University of Ha'il, Saudi Arabia, through project number RG-21008.

### References

- [1] M. Peyrard, S. Cuesta-López, and G. James, "Modelling DNA at the mesoscale: a challenge for nonlinear science?" *Nonlinearity*, vol. 21, no. 6, pp. T91–T100, 2008.
- [2] J. D. Watson and F. H. C. Crick, "Molecular structure of nucleic acids: a structure for deoxyribose nucleic acid," *Nature*, vol. 171, no. 4356, pp. 737–738, 1953.
- [3] L. V. Yakushevich, *Nonlinear Physics of DNA*, John Wiley & Sons, Hoboken, NJ, USA, 2006.
- [4] A. S. Davydov, "Solitons in molecular systems," *Physica Scripta*, vol. 20, no. 3-4, p. 387, 1979.
- [5] S. W. Englander, N. R. Kallenbach, A. J. Heeger, J. A. Krumhansl, and S. Litwin, "Nature of the open state in long polynucleotide double helices: possibility of soliton excitations," *Proceedings of the National Academy of Sciences*, vol. 77, no. 12, pp. 7222–7226, 1980.
- [6] S. Yomosa, "Soliton excitations in deoxyribonucleic acid (DNA) double helices," *Physical Review*, vol. 27, no. 4, pp. 2120–2125, 1983.
- [7] S. Homma and S. Takeno, "A coupled base-rotator model for structure and dynamics of DNA: local fluctuations in helical twist angles and topological solitons," *Progress of Theoretical Physics*, vol. 72, no. 4, pp. 679–693, 1984.
- [8] M. Peyrard and A. R. Bishop, "Statistical mechanics of a nonlinear model for DNA denaturation," *Physical Review Letters*, vol. 62, no. 23, pp. 2755–2758, 1989.
- [9] V. Muto, P. S. Lomdahl, and P. L. Christiansen, "Two-dimensional discrete model for DNA dynamics: longitudinal wave propagation and denaturation," *Physical Review*, vol. 42, no. 12, pp. 7452–7458, 1990.
- [10] L. V. Yakushevich, A. V. Savin, and L. I. Manevitch, "Nonlinear dynamics of topological solitons in DNA," *Physical review. E, Statistical, nonlinear, and soft matter physics*, vol. 66, no. 1, Article ID 016614, 2002.
- [11] D. L. Hien, N. T. Nhan, V. T. Ngo, and N. A. Viet, "Simple combined model for nonlinear excitations in DNA," *Physical review. E, Statistical, nonlinear, and soft matter physics*, vol. 76, no. 2, Article ID 021921, 2007.
- [12] M. Daniel and V. Vasumathi, "Perturbed soliton excitations in the DNA double helix," *Physica D: Nonlinear Phenomena*, vol. 231, no. 1, pp. 10–29, 2007.
- [13] C. B. Tabi, A. Mohamadou, and T. C. Kofané, "Soliton excitation in the DNA double helix," *Physica Scripta*, vol. 77, no. 4, Article ID 045002, 2008.
- [14] S. Zdravković and M. V. Satarčić, "Parameter selection in a peyrard–bishop–dauxis model for DNA dynamics," *Physics Letters A*, vol. 373, no. 31, pp. 2739–2745, 2009.
- [15] G. Gaeta, C. Reiss, M. Peyrard, and T. Dauxois, "Simple models of non-linear DNA dynamics," *La Rivista Del Nuovo Cimento Series 3*, vol. 17, no. 4, pp. 1–48, 1994.
- [16] R. V. Polozov and L. V. Yakushevich, "Nonlinear waves in DNA and regulation of transcription," *Journal of Theoretical Biology*, vol. 130, no. 4, pp. 423–430, 1988.
- [17] J. A. González and M. Martín-Landrove, "Long-range interactions of solitons in a double chain," *Physics Letters A*, vol. 292, no. 4-5, pp. 256–262, 2002.
- [18] L. V. Yakushevich, "Non-linear DNA dynamics and problems of gene regulation," *Nanobiology*, vol. 1, pp. 343–350, 1992.
- [19] K. De-Xing, L. Sen-Yue, and Z. Jin, "Nonlinear dynamics in a new double chain-model of DNA," *Communications in Theoretical Physics*, vol. 36, no. 6, pp. 737–742, 2001.
- [20] W. Alka, A. Goyal, and C. Nagaraja Kumar, "Nonlinear dynamics of DNA—riccati generalized solitary wave solutions," *Physics Letters A*, vol. 375, no. 3, pp. 480–483, 2011.
- [21] A. R. Seadawy, M. Bilal, M. Younis, S. T. R. Rizvi, S. Althobaiti, and M. M. Makhlof, "Analytical mathematical approaches for the double-chain model of DNA by a novel computational technique," *Chaos, Solitons & Fractals*, vol. 144, Article ID 110669, 2021.
- [22] Q. Xian-Min and L. Sen-Yue, "Exact solutions of nonlinear dynamics equation in a new double-chain model of DNA," *Communications in Theoretical Physics*, vol. 39, no. 4, pp. 501–505, 2003.
- [23] Z. Y. Ouyang and S. Zheng, "Travelling wave solutions of nonlinear dynamical equations in a double-chain model of DNA," *Abstract and Applied Analysis*, vol. 2014, Article ID 317543, 5 pages, 2014.
- [24] S. Kumar, A. Kumar, and H. Kharbanda, "Abundant exact closed-form solutions and solitonic structures for the double-chain deoxyribonucleic acid (DNA) model," *Brazilian Journal of Physics*, vol. 51, pp. 1–26, 2021.
- [25] M. E. Elbrolosy and A. A. Elmandouh, "Dynamical behaviour of nondissipative double dispersive microstrain wave in the microstructured solids," *European Physical Journal Plus*, vol. 136, no. 9, pp. 1–20, 2021.
- [26] M. Al Nuwairan and A. A. Elmandouh, "Qualitative analysis and wave propagation of the nonlinear model for low-pass electrical transmission lines," *Physica Scripta*, vol. 96, no. 9, Article ID 095214, 2021.
- [27] A. A. Elmandouh, "Integrability, qualitative analysis and the dynamics of wave solutions for Biswas–Milovic equation," *European Physical Journal Plus*, vol. 136, no. 6, pp. 1–17, 2021.



- [28] A. A. Elmandouh, "Bifurcation and new traveling wave solutions for the 2D Ginzburg-Landau equation," *European Physical Journal Plus*, vol. 135, no. 8, pp. 1–13, 2020.
- [29] M. E. Elbrolosy and A. A. Elmandouh, "Bifurcation and new traveling wave solutions for  $(2+1)$ -dimensional nonlinear Nizhnik-Novikov-Veselov dynamical equation," *European Physical Journal Plus*, vol. 135, no. 6, p. 533, 2020.
- [30] M. E. Elbrolosy, "Qualitative analysis and new soliton solutions for the coupled nonlinear Schrödinger type equations," *Physica Scripta*, vol. 96, no. 12, Article ID 125275, 2021.
- [31] Z.-Y. Zhang, Z.-Y. Liu, X.-J. Miao, and Y.-Z. Chen, "Qualitative analysis and traveling wave solutions for the perturbed nonlinear Schrödinger's equation with Kerr law nonlinearity," *Physics Letters A*, vol. 375, no. 10, pp. 1275–1280, 2011.
- [32] Q.-S. Liu, Z.-Y. Zhang, R.-G. Zhang, and C.-X. Huang, "Dynamical analysis and exact solutions of a new  $(2+1)$ -dimensional generalized boussinesq model equation for nonlinear rossby waves\*," *Communications in Theoretical Physics*, vol. 71, no. 9, p. 1054, 2019.
- [33] P. K. Prasad, A. Abdikian, and A. Saha, "Modeling of nonlinear ion-acoustic solitary, snoidal and superperiodic wave phenomena due to ionospheric escape of Venus," *Advances in Space Research*, vol. 68, no. 10, pp. 4155–4166, 2021.
- [34] A. Abdikian, J. Tamang, and A. Saha, "Supernonlinear wave and multistability in magneto-rotating plasma with  $(r, q)$  distributed electrons," *Physica Scripta*, vol. 96, no. 9, Article ID 095605, 2021.
- [35] K. K. Ali, M. S. Osman, and M. Abdel-Aty, "New optical solitary wave solutions of Fokas-Lenells equation in optical fiber via Sine-Gordon expansion method," *Alexandria Engineering Journal*, vol. 59, no. 3, pp. 1191–1196, 2020.
- [36] K. K. Ali, A.-M. Wazwaz, and M. S. Osman, "Optical soliton solutions to the generalized nonautonomous nonlinear Schrödinger equations in optical fibers via the sine-Gordon expansion method," *Optik*, vol. 208, Article ID 164132, 2020.
- [37] J.-G. Liu, W.-H. Zhu, M. S. Osman, and W.-X. Ma, "An explicit plethora of different classes of interactive lump solutions for an extension form of 3D-Jimbo-Miwa model," *European Physical Journal Plus*, vol. 135, no. 5, p. 412, 2020.
- [38] I. Siddique, M. M. M. Jaradat, A. Zafar, K. Bukht Mehdi, and M. S. Osman, "Exact traveling wave solutions for two prolific conformable M-Fractional differential equations via three diverse approaches," *Results in Physics*, vol. 28, Article ID 104557, 2021.
- [39] X.-I. Miao and Z.-Y. Zhang, "The modified  $G'/G$ -expansion method and traveling wave solutions of nonlinear the perturbed nonlinear Schrödinger's equation with Kerr law nonlinearity," *Communications in Nonlinear Science and Numerical Simulation*, vol. 16, no. 11, pp. 4259–4267, 2011.
- [40] Z. Zhang, J. Huang, J. Zhong et al., "The extended  $(G'/G)$ -expansion method and travelling wave solutions for the perturbed nonlinear Schrödinger's equation with Kerr law nonlinearity," *Pramana*, vol. 82, no. 6, pp. 1011–1029, 2014.
- [41] A. Khalid, A. Rehan, K. S. Nisar, and M. S. Osman, "Splines solutions of boundary value problems that arises in sculpturing electrical process of motors with two rotating mechanism circuit," *Physica Scripta*, vol. 96, 2021.
- [42] S. Kumar, B. Kour, S.-W. Yao, M. Inc, and M. S. Osman, "Invariance analysis, exact solution and conservation laws of  $(2+1)$  dim fractional kadomtsev-petviashvili (KP) system," *Symmetry*, vol. 13, no. 3, p. 477, 2021.
- [43] F. S. Bayones, K. S. Nisar, K. A. Khan et al., "Magneto-hydrodynamics (MHD) flow analysis with mixed convection moves through a stretching surface," *AIP Advances*, vol. 11, no. 4, Article ID 045001, 2021.
- [44] Z. Zhang, "New exact traveling wave solutions for the nonlinear Klein-Gordon equation," *Turkish Journal of Physics*, vol. 32, no. 5, pp. 235–240, 2008.
- [45] Z.-Y. Zhang, Z.-H. Liu, X.-J. Miao, and Y.-Z. Chen, "New exact solutions to the perturbed nonlinear Schrödinger's equation with Kerr law nonlinearity," *Applied Mathematics and Computation*, vol. 216, no. 10, pp. 3064–3072, 2010.
- [46] Z.-Y. Zhang, Y.-X. Li, Z.-H. Liu, and X.-J. Miao, "New exact solutions to the perturbed nonlinear Schrödinger's equation with Kerr law nonlinearity via modified trigonometric function series method," *Communications in Nonlinear Science and Numerical Simulation*, vol. 16, no. 8, pp. 3097–3106, 2011.
- [47] Z. Y. Zhang, J. Zhong, S. S. Dou, J. I. A. O. Liu, D. Peng, and T. I. N. G. Gao, "First integral method and exact solutions to nonlinear partial differential equations arising in mathematical physics," *Romanian Reports in Physics*, vol. 65, no. 4, pp. 1155–1169, 2013.
- [48] Z. Y. Zhang, "Jacobi elliptic function expansion method for the modified Korteweg-de Vries-Zakharov-Kuznetsov and the Hirota equations," *Romanian Journal of Physics*, vol. 60, no. 9-10, pp. 1384–1394, 2015.
- [49] K.-J. Wang, "Generalized variational principle and periodic wave solution to the modified equal width-Burgers equation in nonlinear dispersion media," *Physics Letters A*, vol. 419, Article ID 127723, 2021.
- [50] K. J. Wang, "Abundant analytical solutions to the new coupled Konno-Oono equation arising in magnetic field," *Results in Physics*, vol. 31, Article ID 104931, 2021.
- [51] K.-J. Wang and G.-D. Wang, "Variational theory and new abundant solutions to the  $(1+2)$ -dimensional chiral nonlinear Schrödinger equation in optics," *Physics Letters A*, vol. 412, Article ID 127588, 2021.
- [52] K. J. Wang and G. D. Wang, "Study on the explicit solutions of the Benney-Luke equation via the variational direct method," *Mathematical Methods in the Applied Sciences*, vol. 44, no. 18, pp. 14173–14183, 2021.
- [53] K.-J. Wang, "Periodic solution of the time-space fractional complex nonlinear Fokas-Lenells equation by an ancient Chinese algorithm," *Optik*, vol. 243, Article ID 167461, 2021.
- [54] L. Yang, X. R. Hou, and Z. B. Zeng, "A complete discrimination system for polynomials," *Science in China, Series A*, vol. 39, no. 6, pp. 628–646, 1996.
- [55] L. Cheng-Shi, "Exact travelling wave solutions for  $(1+1)$ -dimensional dispersive long wave equation," *Chinese Physics*, vol. 14, no. 9, pp. 1710–1715, 2005.
- [56] P. F. Byrd and M. D. Fridman, *Handbook of Elliptic Integrals for Engineers and Scientists*, Springer, Berlin, Germany, 1971.
- [57] A. Saha and S. Banerjee, *Dynamical Systems and Nonlinear Waves in Plasmas*, CRC Press, Boca Raton, FL, USA, 2021.